Rare Metal Materials and Engineering
Volume 51, Issue 1, January 2022
Available online at www.rmme.ac.cn

Science Press

Cite this article as: Hu Chen, Chen Li, Zhang Xiao, et al. Effect of SnO_2 Reinforcement Phase on Microstructure and Properties of $AgCuOIn_2O_3$ Electrical Contact Materials[J]. Rare Metal Materials and Engineering, 2022, 51(01): 66-73.

ARTICLE

Effect of SnO_2 Reinforcement Phase on Microstructure and Properties of $AgCuOIn_2O_3$ Electrical Contact Materials

Hu Chen[1], Chen Li[1], Zhang Xiao[1], Li Jintao[1], Liu Manmen[2], Wang Lihui[3], Zhou Xiaolong[1]

[1] Faculty of Materials Science and Engineering, Kunming University of Science and Technology, Kunming 650093, China; [2] Kunming Institute of Precious Metals, Kunming 650106, China; [3] Guilin Key Laboratory of Microelectronic Electrode Materials and Biological Nanomaterials, China Nonferrous Metals (Guilin) Geology and Mining Co., Ltd, Guilin 541004, China

Abstract: $AgCuOIn_2O_3SnO_2$ electrical contact materials with different SnO_2 contents were prepared by reaction synthesis coupled with plastic deformation process. The morphology and microstructure of the $AgCuOIn_2O_3SnO_2$ contact materials were characterized by scanning electron microscopy and optical microscope. The distribution uniformity of the metallographic structure and the reinforcement phase of the materials with different SnO_2 contents was analyzed. The phase structure of the materials was measured by X-ray diffraction, and the tensile strength, hardness, and resistivity of the materials were also measured. Results show that the appropriate SnO_2 addition can significantly decrease the pore size and reduce other defects in the structures. The diffusion of oxides in the silver matrix greatly improves the microstructure uniformity of $AgCuOIn_2O_3$ contact materials. When the SnO_2 content is fixed, the resistivity of materials is decreased with conducting the plastic deformation; with increasing the SnO_2 content, the resistivity is decreased firstly, then increased, and finally turns to be stable at 2.4 μΩ·cm. The hardness of the materials is increased significantly after SnO_2 addition. The material with 1wt% SnO_2 shows the optimal tensile strength and elongation.

Key words: reactive synthesis; $AgCuOIn_2O_3SnO_2$; microstructure; performance

Silver metal oxide electrical contact material has excellent switching characteristics. It is one of the widely used contact materials in low-voltage electrical appliances[1-8]. The universal contact material AgCdO is gradually replaced by AgCuO, $AgSnO_2$, and other contact materials in recent years. AgCuO has better wettability and lower contact resistance, but it has poor resistance to arc erosion and low fusion resistance. Zhou et al[9] studied the microplasticity of CuO particles in AgCuO materials, and found that after superplastic treatment such as extrusion deformation, copper oxide exists in both the monoclinic and cubic crystal phases. The fibrous structure formed by the aggregation of CuO particles appears in the microstructure. The greater the CuO content, the better the electrical contact performance of AgCuO electrical contact material. Xia et al[10] added In to the Ag-Cu system and found that the size of CuO particles after internal oxidation is smaller, and the oxidation degree and arc erosion resistance are significantly improved. $AgSnO_2$ electrical contact materials are resistant to arc erosion and have good resistance against fusion welding. However, due to the poor wettability between Ag and SnO_2, they are easily separated during arc erosion. SnO_2 particles gradually accumulate on the contact surface and increase the contact resistance, thereby resulting in the temperature rise. However, the SnO_2 particles are difficult to process due to their high hardness. Zhou et al[11] used the severe plastic deformation to disperse the agglomerated NiO and SnO_2 particles for preparing a uniformly structured $AgSnO_2NiO$ electrical contact material. Wang et al[12] used Bi_2O_3 as an additive to improve the wettability of $AgSnO_2$ materials.

As electrical contact devices have gradually become precise and miniaturized, the single-phase-reinforced silver-based electrical contact materials can hardly meet the modernization requirements. It is of great significance to study composite

Received date: January 23, 2021
Foundation item: Key Project of Yunnan Province Science and Technology Plan (2017FA027); National Natural Science Foundation of China (51361016)
Corresponding author: Zhou Xiaolong, Ph. D., Professor, Faculty of Materials Science and Engineering, Kunming University of Science and Technology, Kunming 650093, P. R. China, E-mail: kmzxlong@163.com

metal oxide-reinforced silver-based electrical contact materials. Therefore, $AgCuOIn_2O_3SnO_2$ was prepared by reactive synthesis method coupled with plastic deformation process in this research in order to meet the relevant technical standards. X-ray diffractometer (XRD), scanning electron microscope (SEM), and optical microscope (OM) were used to analyze the phase composition and microstructure. The tensile strength, elongation, and other mechanical properties were measured, and the effect of SnO_2 content on the microstructure and mechanical properties of $AgCuOIn_2O_3$ electrical contact materials was discussed.

1 Experiment

The raw materials used for preparing $AgCuOIn_2O_3SnO_2$ electrical contact materials by reaction synthesis method were Ag powder (purity 99%; particle size<45 μm), $AgCu_{20}$ alloy powder (purity 99.5%; particle size<45 μm), $AgIn_{30}$ alloy powder (purity 99.5%; particle size <45 μm), and $AgSn_{15}$ alloy powder (purity 99.5%; particle size<45 μm). The composition of 200 g $AgCuOIn_2O_3SnO_2$ ingot is shown in Table 1. The specimens with 0.2wt%, 0.5wt%, 0.8wt%, and 1.0wt% SnO_2 are named as $AgCuOIn_2O_3$-0.2SnO_2, $AgCuOIn_2O_3$-0.5SnO_2, $AgCuOIn_2O_3$-0.8SnO_2, and $AgCuOIn_2O_3$-1.0SnO_2, respectively.

Firstly, the QM-1SP2 planetary ball mill was used to mix different powders with designed mass, and the mass ratio of ball to powder was 5: 1. The evenly mixed powder was put into a mold of *Φ*26 mm, pressed, and molded under the pressure of 600 MPa. Keep the molded powder at room temperature for 7 min, and then put it into the tubular furnace for sintering. The sintering process was as follows: room temperature→100 °C for 1 h→300 °C for 3 h→500 °C for 3 h →700 °C for 3 h→830 °C for 2 h. After sintering, the ingot and mold were heated to 830 and 350 °C, respectively, and then they suffered pressing under 50 MPa for 5 min, followed by extrusion and drawing. The rivet contacts with diameter of 1.4 mm were obtained.

XRD (D8 ADVANCE, Bruker AXS Company), OM (ECLIPSE MA100N, Nikon), and SEM (TESCAN, Czech Republic) were used. VEGA3 tungsten filament SEM coupled with energy dispersive spectrometer (EDS) was used to analyze the structure and components of the material under back-scattered electron (BSE) and secondary electron (SE) modes. Hardness was measured by HVS-50 digital metal Vickers hardness tester (Shanghai Shangdao SCTMC Company). Tensile strength was measured by AG-IS 10KN universal tester (Shimadzu Company, Japan). Resistance was measured by SB2230 DC resistance tester.

Table 1 Composition of 200 g $AgCuOIn_2O_3SnO_2$ ingot (g)

Specimen	Ag	Ag_2O	$AgCu_{20}$	$AgIn_{30}$	$AgSn_{15}$
$AgCuOIn_2O_3$-0.2SnO_2	37.474	69.510	79.887	11.028	2.101
$AgCuOIn_2O_3$-0.5SnO_2	32.478	71.356	79.887	11.028	5.251
$AgCuOIn_2O_3$-0.8SnO_2	27.482	73.201	79.887	11.028	8.402
$AgCuOIn_2O_3$-1.0SnO_2	24.152	74.430	79.887	11.028	10.503

2 Results and Discussion

2.1 Phase component

As shown in Fig.1, XRD patterns indicate that $AgCuOIn_2O_3SnO_2$ contact materials prepared by the reaction synthesis method contain four phases: Ag, CuO, In_2O_3, and SnO_2. This result indicates that Sn, Cu, and In in the sintered raw materials are oxidized and no other phases are formed.

2.2 Morphology

As shown in Fig. 2, different metal oxides are well distributed in the gray-white silver matrix: the dark-black annular or rod-like structures are CuO; the fine diffused granular and light-gray annular structures are In_2O_3; the gray-black irregular oval annular structures are SnO_2. Based on the diffusion mechanism of the alloy, under the influence of sintering temperature and partial pressure of oxygen, the alloy elements are diffused gradually, react with oxygen to form crystal grains of metal oxide, agglomerate continuously, and finally form the ring oxide structure on the surface edge of the alloy particles. Meanwhile, because the diffusion of alloy elements is slower than that of active oxygen, some oxide particles can also be found inside the annular structures. In order to further verify the formation location and reaction degree of metal oxides, EDS analyses were performed on the structure and structure boundary area, as shown in Fig. 3 and Fig.4, respectively.

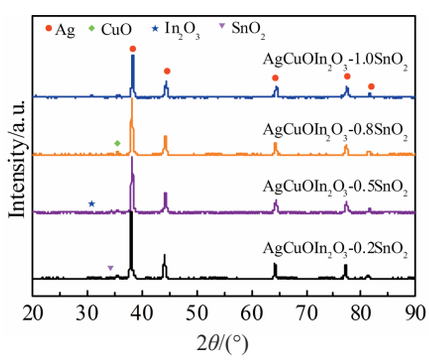

Fig.1 XRD patterns of $AgCuOIn_2O_3SnO_2$ electrical contact materials

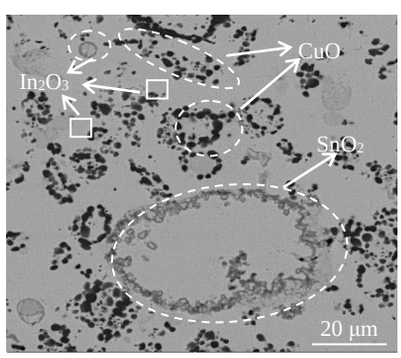

Fig.2 SEM morphology of $AgCuOIn_2O_3SnO_2$ electrical contact material

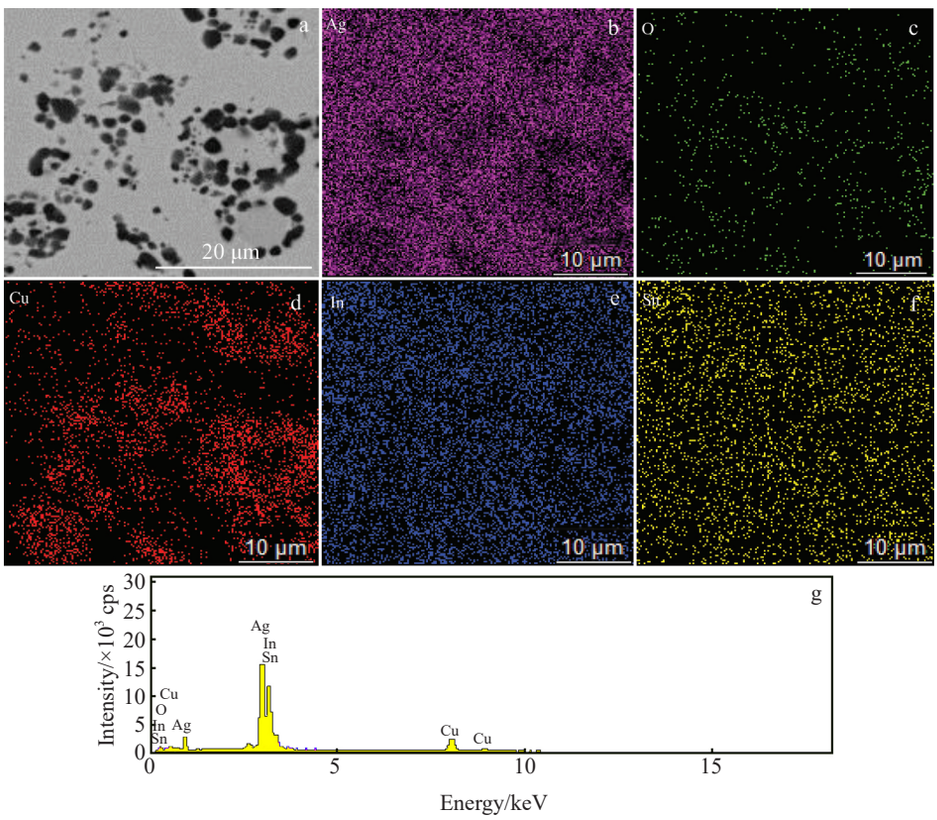

Fig.3 SEM image (a), corresponding EDS element distributions (b~f), and EDS spectrum (g) of structure of $AgCuOIn_2O_3SnO_2$ electrical contact material: (b) Ag, (c) O, (d) Cu, (e) In, and (f) Sn

It can be seen from Fig.3 that the gray white matrix is Ag, and the dark black rod-shaped and annular structure consists of CuO particles. Although In and Sn are dispersed in the silver matrix, no obvious ring structure of In_2O_3 and SnO_2 can be observed in the selected region. Therefore, further analyses were conducted on the ring structure of CuO, junction part of SnO_2, and In_2O_3, as shown in Fig.4

It can be seen from Fig.4 that there is a small amount of Ag in the dark black CuO ring structures, and the oxide particle boundaries are more obvious. Only Ag can be found on the substrate (point 2). The area at point 3 is a silver-oxide particle aggregation area composed of gray-black SnO_2 and Ag. The light gray ring-shaped structure (Fig.4b) consists of In_2O_3 without obvious oxide particle boundaries.

2.3 OM analysis of sintered alloys

Fig. 5 shows the OM microstructures of different $AgCuOIn_2O_3SnO_2$ electrical contact materials after reaction sintering.

It can be seen from Fig.5 that after reaction sintering, metal oxide particles are formed at the boundary and inside the alloy particles, and the particles agglomerate to form the circular structure. These different structure shapes of metal oxides are due to different diffusion rates of each metal in the silver matrix. There are many macro-defects such as pore caused by gas release and impurities in the microstructures of specimens. Furthermore, with increasing the SnO_2 content, the oxides in the structures are more homogeneous and the diffusion is improved. Due to the external conditions, such as the deformation degree and pressure, the interaction of the reinforcement phases in the material can influence the material uniformity.

Fig. 6 shows the OM microstructures of different $AgCuOIn_2O_3SnO_2$ electrical contact materials after pressing and re-sintering. The uniformity of structure distribution of $AgCuOIn_2O_3SnO_2$ specimens is further improved after repressing and re-sintering, and the metal oxides tend to disperse on the silver matrix. The porosity of $AgCuOIn_2O_3$-$0.2SnO_2$ specimen does not decrease significantly, while $AgCuOIn_2O_3$-$0.5SnO_2$ and $AgCuOIn_2O_3$-$0.8SnO_2$ specimens become compact and uniform after repressing and re-sintering. However, in $AgCuOIn_2O_3$-$1.0SnO_2$ specimen, SnO_2 is the brittle phase and its wettability with Ag is poor[13-15], which seriously affects the interface binding strength between metal oxides and Ag, resulting in the large ring structures in the structure. This phenomenon indicates that excessive SnO_2 may adversely affect the structure of $AgCuOIn_2O_3SnO_2$ electrical contact materials.

2.4 OM analysis of plastically-deformed alloys

$AgCuOIn_2O_3$-$0.5SnO_2$ and $AgCuOIn_2O_3$-$1.0SnO_2$ alloys after extrusion process (Φ6 mm at initial state; Φ3.4 mm at intermediate state; Φ1.4 mm at final state) were investigated, and the influence of different SnO_2 contents and plastic deformation on the microstructures was analyzed. Fig.7 shows

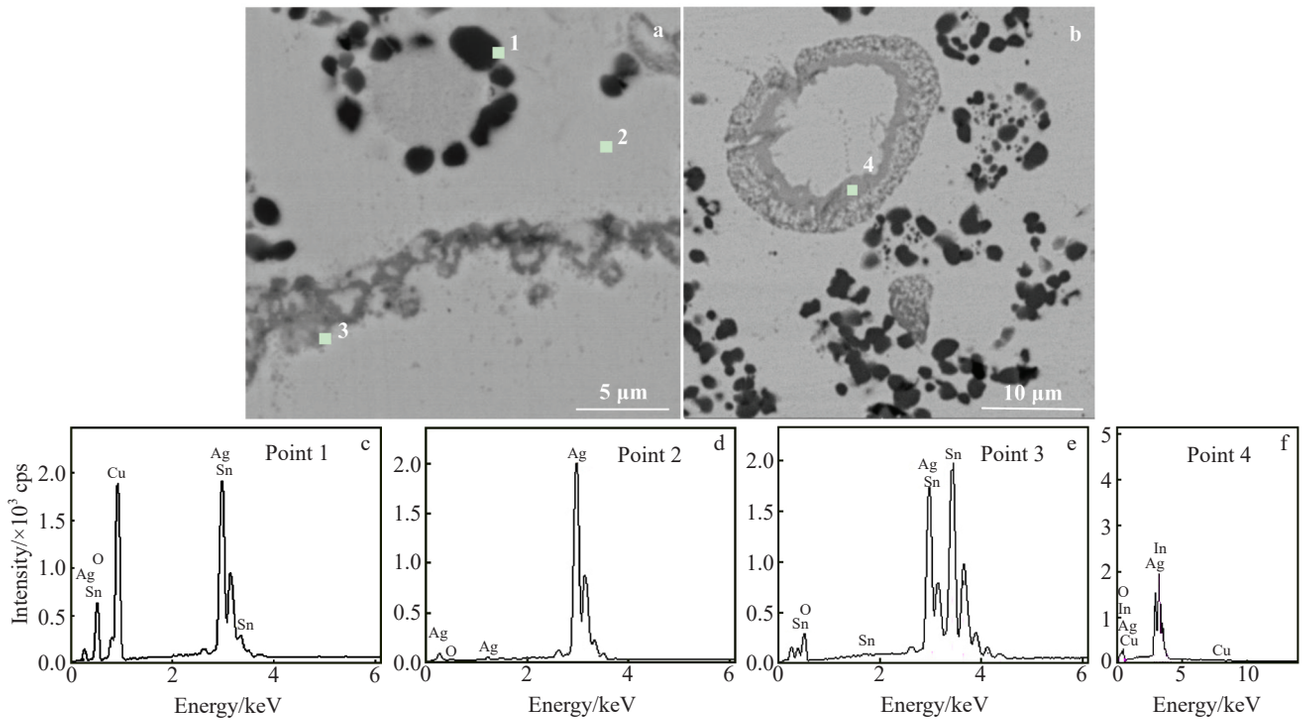

Fig.4 SEM images of $AgCuOIn_2O_3SnO_2$ electrical contact material (a, b); EDS spectra of point 1 (c), point 2 (d), and point 3 (e) in Fig.4a and point 4 (f) in Fig.4b

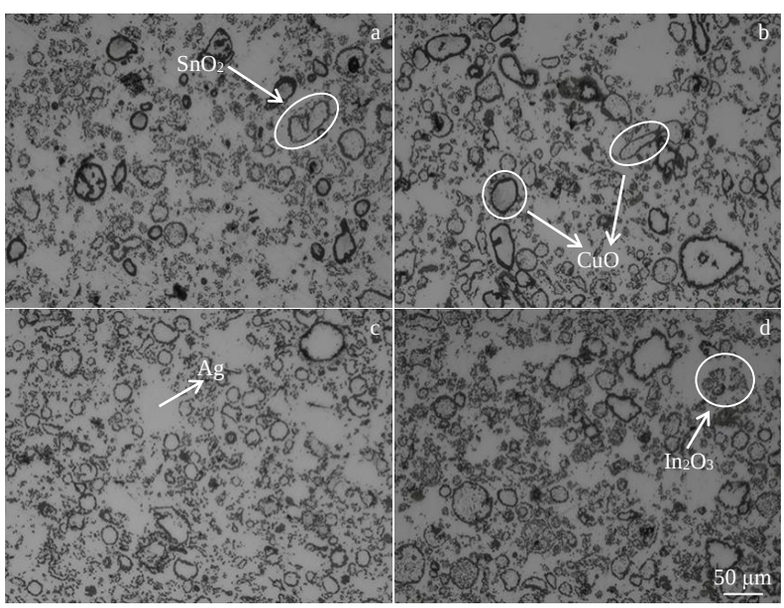

Fig.5 OM microstructures of $AgCuOIn_2O_3$-$0.2SnO_2$ (a), $AgCuOIn_2O_3$-$0.5SnO_2$ (b), $AgCuOIn_2O_3$-$0.8SnO_2$ (c), and $AgCuOIn_2O_3$-$1.0SnO_2$ (d) electrical contact materials after reaction sintering

the transverse OM microstructures of $AgCuOIn_2O_3SnO_2$ electrical contact materials after hot extrusion and cold drawing.

It can be seen that larger annular structure of CuO particles (circle regions in Fig. 7a and 7b) exist in the $AgCuOIn_2O_3$-$0.5SnO_2$ and $AgCuOIn_2O_3$-$1.0SnO_2$ alloys, and In_2O_3 and SnO_2 particles are dispersed in the silver matrix. The structure distribution is more uniform than that of the sintered specimens, but there are still pits, voids, and other defects. Besides, the porosity of $AgCuOIn_2O_3$-$1.0SnO_2$ alloy is significantly larger than that of $AgCuOIn_2O_3$-$0.5SnO_2$ alloy. After cold-drawing treatment, the microstructure becomes fine and uniform, the dispersive distribution of metal oxide particles can be observed, and the macro-defects such as holes are significantly reduced. Obviously, the $AgCuOIn_2O_3$-$0.5SnO_2$ alloy has uniform transverse structure and better

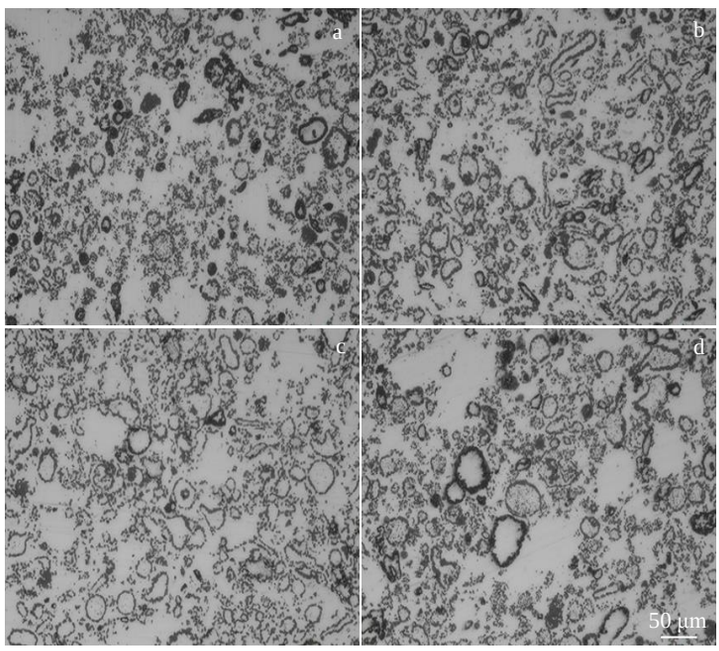

Fig.6 OM microstructures of $AgCuOIn_2O_3$-0.2SnO_2 (a), $AgCuOIn_2O_3$-0.5SnO_2 (b), $AgCuOIn_2O_3$-0.8SnO_2 (c), and $AgCuOIn_2O_3$-1.0SnO_2 (d) electrical contact materials after repressing and re-sintering

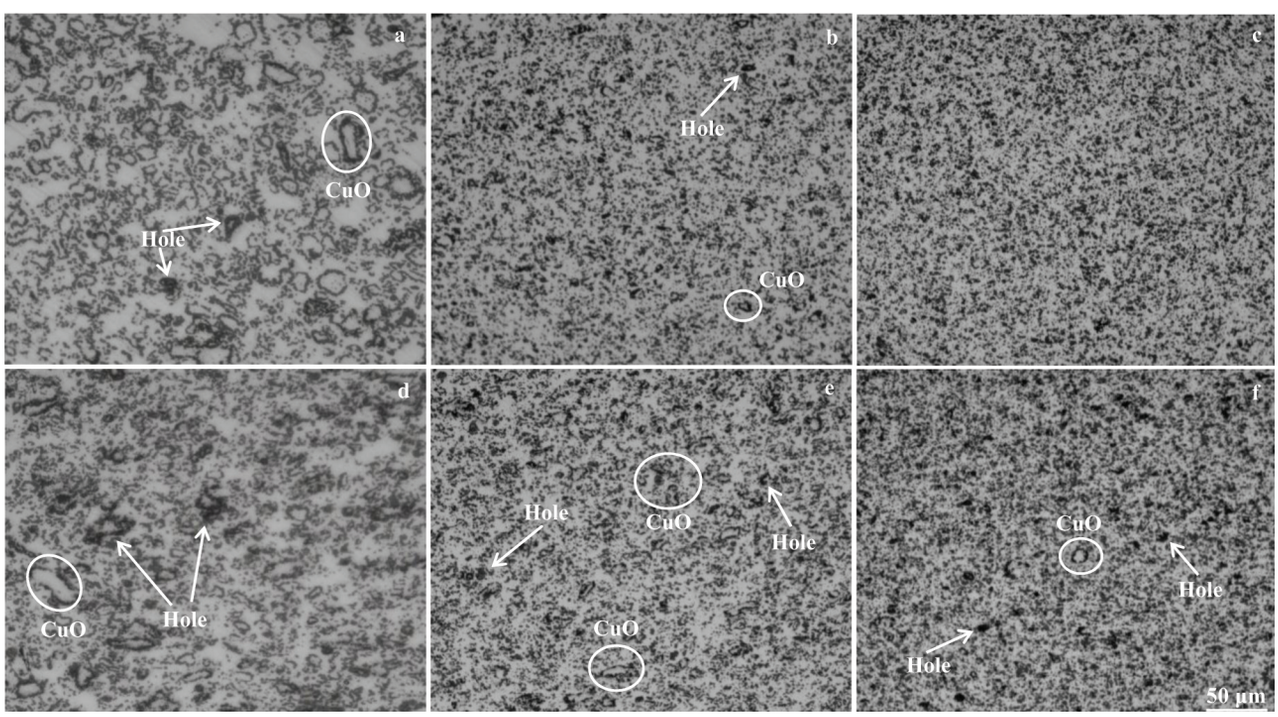

Fig.7 Transverse OM microstructures of $AgCuOIn_2O_3$-0.5SnO_2 (a~c) and $AgCuOIn_2O_3$-1.0SnO_2 (d~f) alloys in extrusion process: (a, d) Φ6 mm at initial stage, (b, e) Φ3.4 mm at intermediate stage, and (c, f) Φ1.4 mm at final stage

integrity than $AgCuOIn_2O_3$-1.0SnO_2 alloy does.

Fig. 8 shows the longitudinal OM microstructures of $AgCuOIn_2O_3SnO_2$ electrical contact materials after hot extrusion and cold drawing. It can be found that after hot extrusion treatment, the fibrous CuO structure appears along the extrusion direction, which is consistent with the structure of AgCuO composite after hot extrusion. Compared with $AgCuOIn_2O_3$-0.5SnO_2 specimen, the $AgCuOIn_2O_3$-1.0SnO_2 specimen has larger fibrous CuO with larger and more dispersed structures, as indicated by the elliptical areas in

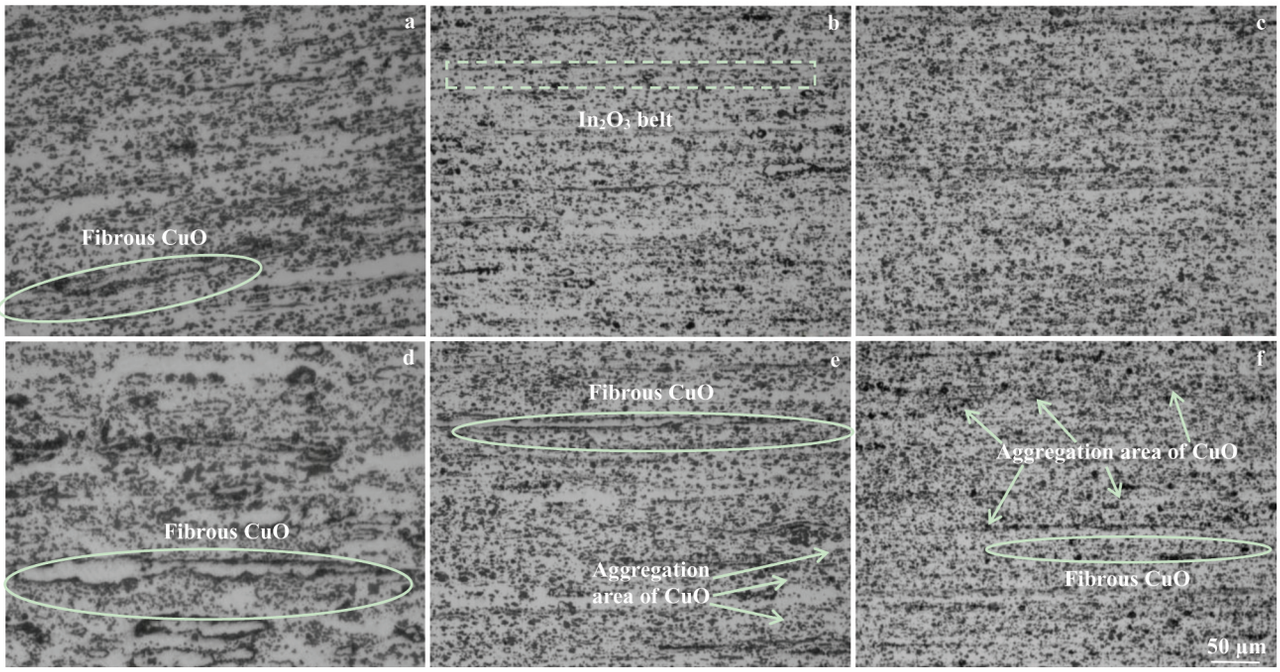

Fig.8 Longitudinal OM microstructures of $AgCuOIn_2O_3$-0.5SnO_2 (a~c) and $AgCuOIn_2O_3$-1.0SnO_2 (d~f) alloys in extrusion process: (a, d) *Φ*6 mm at initial state, (b, e) *Φ*3.4 mm at intermediate state, and (c, f) *Φ*1.4 mm at final state

Fig. 8a and 8d. The light gray In_2O_3 band structure can be found in the specimens at the intermediate state which is associated with the fibrous CuO. In addition, the formation of CuO in $AgCuOIn_2O_3$-0.5SnO_2 specimen is due to the diffusion and growth of CuO phase, which undermines the structure homogeneity. As the cold drawing proceeds, the metal oxide structure becomes gradually compressed, broken, and dispersed, and it is eventually arranged in an orderly linear structure along the drawing direction. Meanwhile, the longitudinal homogeneity of $AgCuOIn_2O_3$-0.5SnO_2 specimen is better than that of $AgCuOIn_2O_3$-1.0SnO_2 specimen. In general, after plastic deformation treatment, the $AgCuOIn_2O_3$-SnO_2 electrical contact materials have a more uniform distribution of particles and structures, resulting in the dispersion strengthening effect which has a significant influence on the tensile strength, elongation, and the resistivity.

2.5 Microstructure

The microstructure of $AgCuOIn_2O_3$ and $AgCuOIn_2O_3SnO_2$ alloys was investigated and compared. The OM morphologies of $AgCuOIn_2O_3$ material are shown in Fig.9

It can be seen that the $AgCuOIn_2O_3$ specimen at the final extrusion state (*Φ*1.4 mm) has obvious pits and pores, and the In_2O_3 particles are agglomerated, forming a large area. Compared with the microstructures of $AgCuOIn_2O_3$-0.5SnO_2 specimen (Fig.7c and Fig.8c), it can be found that the addition of SnO_2 can reduce the agglomeration of In_2O_3 particles, and the metal oxide particles are dispersed more homogeneously in the silver matrix.

2.6 Mechanical properties

Strength and plasticity are important components of the mechanical properties of electrical contact materials, which affect their service life and mechanical wear resistance. The

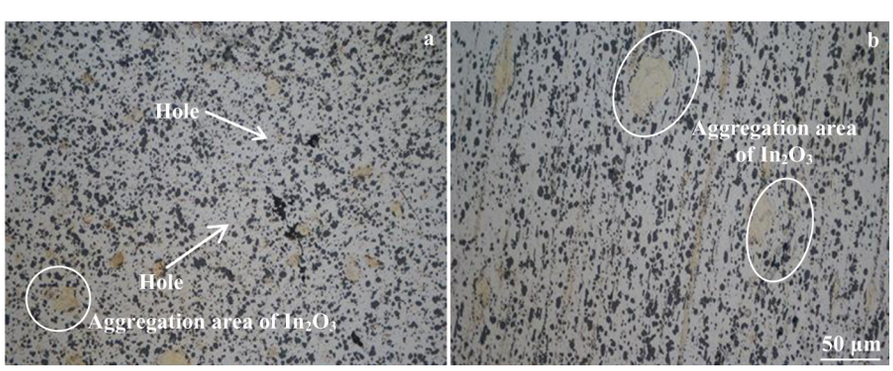

Fig.9 Longitudinal (a) and transverse (b) microstructures of $AgCuOIn_2O_3SnO_2$ alloy after extrusion

results of tensile strength and elongation of different $AgCuOIn_2O_3SnO_2$ electrical contact materials after the tensile tests at room temperature are shown in Fig.10.

It can be seen that with increasing the SnO_2 content, the tensile strength of $AgCuOIn_2O_3SnO_2$ electrical contact materials is gradually improved, and the elongation is decreased slightly and then increased. When the SnO_2 content increases from 0.2wt% to 0.5wt% , the tensile strength increases rapidly. The $AgCuOIn_2O_3$-1.0SnO_2 specimen has the highest tensile strength (219.268 MPa) and the largest elongation (20.2%). The $AgCuOIn_2O_3$-0.2SnO_2 specimen has the lowest tensile strength (193.107 MPa) and relatively small elongation (17.2%).

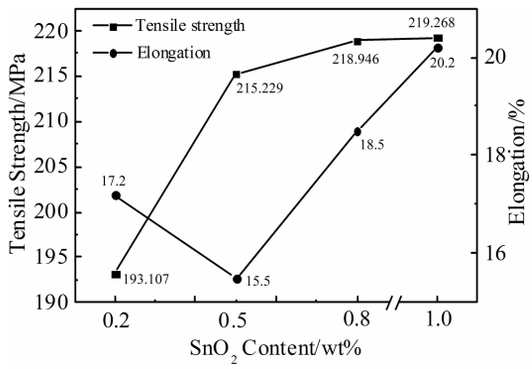

Fig.10 Mechanical properties of different $AgCuOIn_2O_3SnO_2$ electrical contact materials

2.7 Hardness

The hardness of different $AgCuOIn_2O_3SnO_2$ electrical contact materials is shown in Fig. 11. It can be seen that the Vickers hardness of sintered specimens is low, and is significantly improved after re-sintering process. The hardness of the re-sintered specimens is gradually increased with increasing the content of brittle phase SnO_2. At the initial stage of plastic deformation, the hardness of specimens with different SnO_2 contents is similar. As the deformation proceeds, the hardness of four specimens is quite different. In particular, the hardness of $AgCuOIn_2O_3$-0.5SnO_2 and $AgCuOIn_2O_3$-1.0SnO_2 specimens drops sharply to about 600 MPa. The $AgCuOIn_2O_3$-0.5SnO_2 specimen has the lowest hardness, indicating that this alloy is suitable for manufacture of finished rivets.

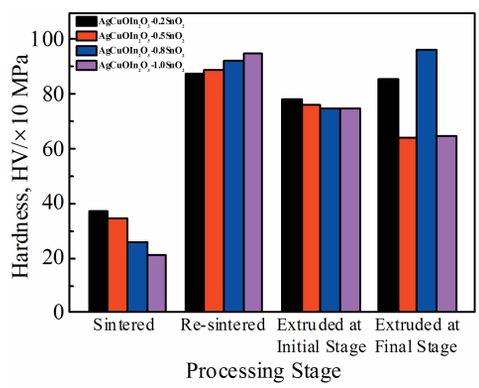

Fig.11 Hardness of different $AgCuOIn_2O_3SnO_2$ electrical contact materials at different processing stages

2.8 Conductivity

It can be seen from Table 2 that the resistivity of the specimens after reaction sintering is high, and the repressing and re-sintering processes can significantly reduce the resistivity of the $AgCuOIn_2O_3SnO_2$ electrical contact material. As the SnO_2 content increases, the total oxide content increases. Due to the poor conductivity of the oxide, the resistivity of specimens is firstly decreased, then increased, and finally tends to be a constant at around 2.4 μΩ·cm with increasing the SnO_2 content.

Table 2 Resistivity of $AgCuOIn_2O_3SnO_2$ electrical contact materials in different processing states (μΩ·cm)

Specimen	Sintered	Re-sintered	Plastically deformed				
			*Φ*6.0 mm	*Φ*5.2 mm	*Φ*3.4 mm	*Φ*2.2 mm	*Φ*1.4 mm
$AgCuOIn_2O_3$-0.2SnO_2	4.673	2.857	2.244	2.161	2.328	2.326	2.367
$AgCuOIn_2O_3$-0.5SnO_2	5.051	3.030	2.387	2.211	2.312	2.354	2.378
$AgCuOIn_2O_3$-0.8SnO_2	5.682	3.077	2.545	2.246	2.362	2.375	2.407
$AgCuOIn_2O_3$-1.0SnO_2	6.494	3.030	2.618	2.279	2.373	2.375	2.419

3 Conclusions

1) The phase components of $AgCuOIn_2O_3SnO_2$ electrical contact materials prepared by reaction synthesis include Ag, CuO, In_2O_3, and SnO_2 phases.

2) After repressing, resintering, and hot extrusion, the distribution uniformity of microstructures is improved significantly and the hardness is increased compared with those of sintered $AgCuOIn_2O_3SnO_2$ alloys.

3) After plastic deformation treatment, the $AgCuOIn_2O_3SnO_2$ electrical contact materials acquire a more uniform distribution of particles and structures, resulting in the dispersion strengthening effect which has a significant influence on the tensile strength, elongation, and the resistivity.

4) With increasing the SnO_2 content of $AgCuOIn_2O_3SnO_2$ electrical contact materials, the microstructures of the specimens are more uniform, and the reinforced phase particles are dispersed in the silver matrix. Compared with that of $AgCuOIn_2O_3$ alloy, the aggregation degree of In_2O_3 particles of prepared alloys is significantly reduced.

References

1 Timsit R S. *Electrical Contact Materials*[M]. New York: Springer, 2013

2 Ding C, Li C X, Fang C H. *IEEJ Transactions on Electrical & Electronic Engineering*[J], 2020, 15(2): 187

3 Joshi P B, Murti N S S, Gadgeel V L *et al*. *Journal of Materials Science Letters*[J], 1995, 14(16): 1099

4 Wang J, Feng Y, Li S *et al*. *Transactions of Nonferrous Metals Society of China*[J], 2009, 19(1): 113

5 Lin X Y, Hao H T, Xie M. *Materials Science Forum*[J], 2019, 953: 115

6 Jeannot D, Pinard J, Ramoni P *et al. IEEE Transactions on Components, Packaging, and Manufacturing Technology: Part A* [J], 1994, 17(1): 17

7 Clary D R, Mills G. *The Journal of Physical Chemistry C*[J], 2011, 115(5): 1767

8 Swingler J, McBride J W. *IEEE Transactions on Components, Packaging, and Manufacturing Technology: Part A*[J], 1996, 19(3): 404

9 Zhou Xiaolong, Cao Jianchun, Chen Jingchao *et al*. *Rare Metal Materials and Engineering*[J], 2013, 42(11): 2242

10 Xia Jing, Xiang Xiongzhi, Hu Xugao *et al. Precious Metals*[J], 2014, 35(3): 35 (in Chinese)

11 Zhou Xiaolong, Xiong Aihu, Liu Manmen *et al*. *Rare Metal Materials and Engineering*[J], 2019, 48(9): 2885 (in Chinese)

12 Wang Haitao. *Thesis for Master*[D]. Tianjin: Hebei University of Technology, 2007 (in Chinese)

13 Wang Jiazhen, Wang Yaping, Yang Zhimao *et al*. *Rare Metal Materials and Engineering*[J], 2005, 34(3): 405 (in Chinese)

14 Li Guijing, Yang Tianyang, Ma Yuanyuan *et al*. *Ceramics International*[J], 2020, 46(4): 4897

15 Taha M A, Zawrah M F. *Ceramics International*[J], 2017, 43(15): 12 698

SnO_2增强相对$AgCuOIn_2O_3$电触头材料显微组织与性能的影响

胡　晨[1]，陈　力[1]，张　晓[1]，李金涛[1]，刘满门[2]，王丽慧[3]，周晓龙[1]

(1. 昆明理工大学 材料科学与工程学院，云南 昆明 650093)

(2. 稀贵金属综合利用新技术国家重点实验室，云南 昆明 650106)

(3. 中国有色桂林矿产地质研究院有限公司 桂林市微电子元件电极材料与生物纳米材料重点实验室，广西 桂林 541004)

摘　要：采用反应合成法结合塑性变形工艺制备了不同SnO_2含量的$AgCuOIn_2O_3SnO_2$电触头材料，利用扫描电镜和金相显微镜表征了材料的微观形貌及显微组织，分析对比了不同SnO_2含量的材料金相组织及其增强相的分布均匀性，并利用X射线衍射分析了材料的物相结构。测量了材料的抗拉伸强度、硬度、电阻等性能。结果表明：添加适量的SnO_2能使组织中的孔隙尺寸缩小、其他缺陷明显减少。氧化物弥散分布在银基体中，极大地改善了$AgCuOIn_2O_3$电触头材料的显微组织均匀性。在SnO_2含量不变时，材料的电阻率随塑性变形程度增加而有所降低；随着SnO_2含量增多，电阻率呈现先降低后升高的趋势，最后趋于定值，约为2.4 μΩ·cm。添加SnO_2后各试样材料的硬度均显著升高，SnO_2含量为1%（质量分数）的材料具有最优的抗拉伸强度和延伸率。

关键词：反应合成法；$AgCuOIn_2O_3SnO_2$；显微组织；性能

作者简介：胡　晨，男，1997年生，硕士，昆明理工大学材料科学与工程学院，云南 昆明 650093，E-mail：1069661438@qq.com